J Porous Mater (2006) 13: 73–80
DOI 10.1007/s10934-006-5492-4

Template-assisted syntheses of porous metal methylphosphonates

Zongbin Wu · Jingcheng Tian · Zhongmin Liu · Peng Tian · Lei Xu · Yue Yang · Yangyang Zhang · Xinhe Bao · Xiumei Liu · Xianchun Liu

Received: January 7, 2004 / Revised: August 2, 2005

Abstract Neutral dibutyl methylphosphonate (DBMP) is used as a template to prepare porous metal methylphosphonates (metal = aluminum, titanium, zirconium). The removal of DBMP in the as-synthesized materials could be easily achieved by evaporation under vacuum without destroying the hybrid structure, as evidenced by elemental analyses, FT-IR spectra, ^{13}C CP/MAS NMR and nitrogen adsorption-desorption isotherms. Thermal analyses show that three porous hybrid samples have high thermal stability in air. The exothermic weight losses due to oxidation combustion of organic species occluded in samples appear after 730 K. Furthermore, the templating effect of DBMP is also confirmed by comparing the hybrid materials synthesized in the presence or the absence of the template.

Keywords Dibutyl methylphosphonate · Template-assisted synthesis · Porous material · Metal methylphosphonate

1. Introduction

Organic-inorganic hybrid porous materials have recently received great attraction. The research in the area mainly focuses on the following subjects: (1) the synthesis, characterization and structural determination of new organic-inorganic hybrid porous materials; (2) the formation mechanism; (3) the application of novel materials in the fields of catalysis, sorption, storage, and so on [1–3]. Currently, the exploration of new synthetic methods and synthesis of materials with novel structures are of high significance.

Undoubtedly, direct synthesis of porous coordination polymer is a simple and efficient method to obtain organic-inorganic hybrid porous materials. Therefore, porous coordination polymer is a vogue concept in the field. On the basis of the principle of coordination chemistry, crystal engineering and supramolecular synthesis, many novel porous coordination polymers have been designed and synthesized successfully [3]. However, since only a few of them exhibit accessible and utilizable porosities, the new concept is undergoing the examination of actual effects.

Another approach is referred to the template-assisted method, which has played an important role in the field of inorganic porous materials [4–6]. Zeolites, as the most typical inorganic porous materials, were first synthesized hydrothermally with hydrated alkali or alkaline earth metal cations as the templates. Subsequently, the use of quaternary ammonium cations created a new era of zeolite synthesis [4, 7, 8]. Up to date, various microporous zeolites with a wide range of compositions and structures have been prepared under hydrothermal condition from gels or solutions containing organic ions (e.g. ammonium salts) or organic molecules (e.g. amines) as the templates. The templateing molecules, possibly acting as structure-directing agents, charge-compensating agents or space-filling agents, favour the formation of porous structures during the crystallization. However, the micropore sizes of classic zeolites seriously hinder the diffusion of larger molecules inside channels, which arouses the

Z. Wu · Z. Liu (✉) · P. Tian · L. Xu · Y. Yang · Y. Zhang
Natural Gas Utilization & Applied Catalysis Laboratory, Dalian Institute of Chemical Physics, Chinese Academy of Sciences, P.O. Box 110, Dalian 116023, P. R. China
e-mail: liuzm@dicp.ac.cn

J. Tian
Department of Biochemistry and Environment Engineering, Jiaozuo University, Jiaozuo 454003, P. R. China

X. Bao · Xiumei Liu · Xianchun Liu
State Key Laboratory of Catalysis, Dalian Institute of Chemical Physics, Chinese Academy of Sciences, P.O. Box 110, Dalian 116023, P. R. China

interest of developing mesoporous or macroporous materials. The first success was indebted to the discovery of silica-based mesoporous molecular sieves (denoted as MCM-41) templated by long-chain quaternary ammonium surfactants [9]. Thereafter, based on the liquid-crystal templating mechanism many nonsilica-based mesoporous oxides were synthesized as well [10, 11]. Additionally, polymers could be used as templates to synthesize macroporous materials [5]. Zeolite itself could also take templating effects on the formation of ordered carbon molecular sieves and vice versa. The experimental results showed that the thus-obtained structures were not a simple negative replica of the templates used and the synthesis mechanism involved a structural transformation triggered by the removal of the template [12, 13, 14].

For those inorganic porous materials prepared by the above-mentioned routes, the templates occluded inside channels can be removed by extraction or calcinations. However, for organic-inorganic hybrid porous materials, it is very difficult to take the same techniques to remove the templates without destroying the host porous structures. This is the main reason why the template-assisted method has not been widely employed in the field. The obstacle prompts the pursuit of new templates and novel host-guest interactions for reviving the template-assisted method in the field of organic-inorganic hybrid porous materials. Recently, the work on vanadium alkylphosphonate revealed that small alcohol could help to create well-defined micropores, and that the resulting micropores could recognize primary alcohol molecules and selectively discriminate among various branched isomers [15, 16].

Very recently, we reported the application of neutral dibutyl methylphosphonate (DBMP) as the template to assemble mesoporous aluminum methylphosphonate (AMPF), in which DBMP could be removed through the treatment at 673 K under the pressure of 10 mmHg [17]. The present work reports further detailed investigations on the synthesis of porous zirconium and titanium methylphosphonates templated by DBMP. The porous structures of obtained samples were determined by N_2 physisorption experiments. FT-IR spectra, ^{13}C CP/MAS NMR and thermal analyses were employed to investigate the removal process of DBMP from the as-synthesized materials and the thermal stability of the final porous samples. In addition, the templating effect of DBMP was elucidated by comparing the hybrid materials synthesized with or without the template-assisted method.

2. Experimental

2.1. Materials

The analytical reagents used for the synthesis included aluminum nitrate ($Al(NO_3)_3 \cdot 9H_2O$), titanium (IV) butoxide ($Ti(C_4H_9O)_4$), zirconium nitrate ($Zr(NO_3)_4 \cdot 5H_2O$), acetonitrile (CH_3CN), and benzene (C_6H_6). A mixture (designated as DMM) of DBMP and MPA (CH_3PO_3, methylphosphonic acid) was prepared according to the previous report [17]. ^1H NMR, GC-MS and elemental analyses showed the molar ratio of MPA: DBMP = 1.3: 1 in DMM.

2.2. Preparation of porous metal methylphosphonates with template-assisted method

AMPF (mesoporous aluminum methylphosphonate): The synthesis procedure has been described in detail elsewhere [17]. AMPF was obtained by treating the as-synthesized aluminum methylphosphonate (designated as AMP) at 673 K and 10 mmHg for 2 h to remove the template DBMP. Elemental analysis of AMPF gave the following composition (wt%): C 11.24, H 3.28, Al 10.39, and P 28.80.

TiMPF (microporous titanium methylphosphonate): 23.8 ml of titanium (IV) butoxide was added into 60 ml of acetonitrile under stirring at room temperature. After 10 min, 16 ml of DMM was added and the mixture was stirred for 30 min. 150 ml of benzene was added into the above mixture and kept stirring for another 30 min. A white precipitate was formed as soon as 500 ml of deionized water was poured into the mixture. The precipitate congregated and floated in the interface between water and organic mixture, when stirring was stopped. The product was centrifuged, washed with deionized water for three times, and dried at 343 K (1.5 mmHg) to produce the as-synthesized titanium methylphosphonate (designated as TiMP). Elemental analysis of TiMP gave the following composition (wt%): C 23.34, H 5.07, P 18.3, and Ti 14.0 (yield 91%, based on Ti).

TiMPF was obtained by removing the template of TiMP at 573 K for 4 h at the pressure of 2×10^{-2} mmHg. Elemental analysis of TiMPF gave the following composition (wt%): C 11.87, H 2.89, P 30.07, and Ti 18.4 (the yield: 93%, based on Ti).

ZrMPF (microporous zirconium methylphosphonate): The synthesis procedure was similar with that of TiMP except for 30 gram of zirconium nitrate as the metal precusor. Elemental analysis of the as-synthesized zirconium methylphosphonate (designated as ZrMP) gave the following composition (wt%): C 13.2, H 4.6, P 7.5, and Zr 35.2 (yield 95%, based on Zr).

After ZrMP was treated at 573 K and 2×10^{-2} mmHg for 4 h to remove the template, ZrMPF was formed. Elemental analysis of ZrMPF gave the following composition (wt%): C 5.4, H 1.6, P 7.1, and Zr 55.1 (yield 90%, based on Zr).

2.3. Preparation of metal methylphosphonates (AMPcon, TiMPcon, and ZrMPcon) as control samples without using template-assisted method

AMPcon (as control sample of aluminum methylphosphonate) was prepared based on the synthesis procedure of

AMPF, in which 3.44 g of MPA in place of 8 ml DMM was added. The synthesis of TiMPcon (as control sample of titanium methylphosphonate) was conducted using the procedure similar to that of TiMPF, but adding 6.88 g of MPA instead of 16 ml DMM. Similarly, ZrMPcon (as control sample of zirconium methylphosphonate) was synthesized using the same synthetic process as that of ZrMPF, but adding 6.88 g of MPA in place of 16 ml DMM.

2.4. Characterization

^{13}C CP/MAS NMR (MAS, magic angle spinning) was recorded at room temperature on a Bruker DRX-400 Spectrometer with BBO MAS probe at a magnetic field of 9.4T, with a resonance frequency of 128.4 MHz. The spinning rate of the samples was kept at 4 KHz for ^{13}C. The chemical shift was referenced to a saturated aqueous solution of sodium 4, 4-dimethyl-4-silapentane sulfonate (DSS).

FTIR spectra were measured on a Bruker EQUINOX 55 FTIR spectrometer with a resolution of 4 cm^{-1}. In order to investigate the process of template removal and the thermal stability of hybrid structures of metal methylphosphonates, an *in-situ* cell equipped with ZnSe windows (Spectra-Tech) was used for those experiments performed at high temperatures and low pressures. The pellet of pure sample was first put into the cell and heated at different temperatures for a certain time, and then cooled down to ambient temperature naturally under vacuum. All spectra were recorded at ambient temperature. The samples of TiMP and ZrMP were treated at each temperature for 30 min at the pressure of 2×10^{-2} mmHg, whereas the treatment of AMP was carried out at the given temperature for 2 h at 10 mmHg.

Nitrogen adsorption-desorption isotherms were measured on a Micromeritics ASAP-2010 apparatus at 77.35 K. Prior to the measurements, all the samples were outgassed at 523 K for 6 h. Specific surface areas of the materials under study were calculated using the BET method. Both microporosity and mesoporosity were evaluated according to high-resolution α_s plots [18, 19]. An octyldimethylsilyl (ODMS)-modified LiChrospher Si-1000 Silica (RO1) was used as reference adsorbent [20]. Pore size distributions (PSD) for the samples were calculated using the Horvath-Kawazoe (HK) and Density Functional Theory (DFT) models. The softwares were provided by Micromeritics Instrument Corporation.

Thermogravimetric (TG) and differential thermal analysis (DTA) measurements were separately recorded on a Perkin Elmer Pyriss TGA and a Perkin Elmer DTA7 equipment, ranging from 323 K to 1173 K with a heating rate of 10 K/min under air flow of 20 ml/min.

3. Results and discussion

3.1. Characterization of porous metal methylphosphonates

3.1.1. Nitrogen adsorption-desorption isotherm

The specific surface area and porosity of AMPF, TiMPF and ZrMPF samples are characterized by N_2 physisorption. The N_2 adsorption-desorption isotherm of each sample and its corresponding α_s plot are presented in Fig. 1. The structural parameters for all the samples are collected in Table 1.

Type I nitrogen isotherms are observed for TiMPF and ZrMPF (Fig. 1 (a) and (b)), indicating that both are

Table 1 Structural parameters calculated by BET, α_s-plots, HK, and DFT methods

Sample	$S_{BET}^{(a)}$ ($m^2\cdot g^{-1}$)	$S_{mi}^{(b,c)}$ ($m^2\cdot g^{-1}$)	$S_{me}^{(b)}$ ($m^2\cdot g^{-1}$)	$S_{ext}^{(b)}$ ($m^2\cdot g^{-1}$)	$V_{tot}^{(b)}$ ($cm^3\cdot g^{-1}$)	$V_{mi}^{(b)}$ ($cm^3\cdot g^{-1}$)	$V_{me}^{(d)}$ ($cm^3\cdot g^{-1}$)	$W^{(e)}$ (nm)
TiMPF	290	287	0	3	0.15	0.15	0	0.56
TiMPcon	2	–	–	–	–	–	–	–
ZrMPF	279	254	0	20	0.13	0.13	0	0.58
ZrMPcon	314	144	29	96	0.11	0.09	0.02	1.2
AMPF	90	0	90	0	0.32	0	0.32	12
AMPcon	11	–	–	–	–	–	–	–

[(a)]Calculated by BET method.

[(b)]Calculated by α_s-plots method; S_{me} refers to the surface area of order mesopores and S_{ext} refers to the surface area of textural mesopores.

[(c)]$S_{mi} = S_{BET} - S_{me} - S_{ext}$.

[(d)]$V_{tot} = V_{mi} + V_{me}$.

[(e)]the maximum of PSD calculated by HK (TiMPF and ZrMPF) or DFT method (AMPF and ZrMPcon).

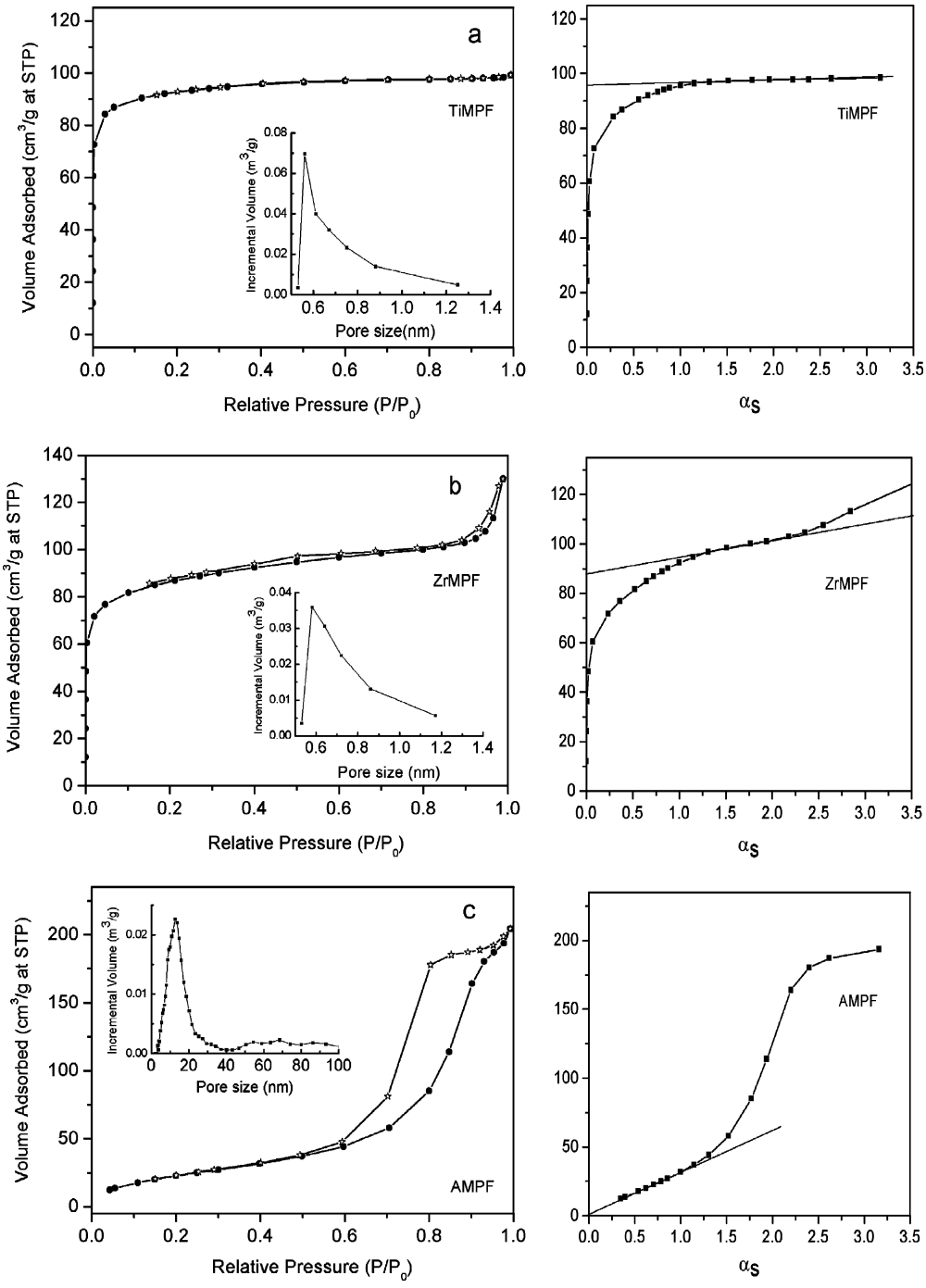

Fig. 1 N_2 adsorption-desorption isotherms (● adsorption, ✡ desorption), pore size distribution (inset, a and b by HK method, c by DFT method) and α_s plots of porous samples

microporous materials [21]. Their α_s plots exhibit typical filling swings due to the enhanced surface-molecule interactions, which suggests the presence of micropores with the size less than 1.0 nm in the samples [22]. This is also confirmed by the pore size distributions (PSD) calculated from nitrogen adsorption branches using the HK model based on the slit pore geometry. The profiles of PSD show the maxima at 0.56 nm for TiMPF and 0.58 nm for ZrMPF. The α_s plots of the two materials have a linear region in the range of $1.0 < \alpha_s < 2.25$. Microporous volume (V_{mi}) and extra surface area (S_{ext}) can be calculated from the intercept and slope of the linear region (see Table 1) [22].

AMPF sample presents a *Type IV* isotherm with a *Type I* hysteresis loop, characteristic of mesoporous materials with a symmetrical and narrow pore size distribution concentrated at 12 nm, calculated by using the DFT model. Moreover, the

absence of filling swing in the α_s plot of AMPF reveals that there is no any micropore in the structure. The α_s plot is linear in the low-pressure range, from which the total specific surface area is calculated to be 90 m^2/g, in good agreement with the value obtained by BET method.

3.1.2. FT-IR

FT-IR was used to investigate the removal process of DBMP from the as-synthesized metal methylphosphonates (TiMP, ZrMP and AMP). Fig. 2 shows the IR spectra of three samples after thermal treatment at different temperatures under vacuum.

With the increase of temperature, the intensity of the bands assigned to methyl, methene and methine groups in DBMP (2959, 2933, 2873, 2843, 1466, 1460, 1380 cm^{-1}) decreases gradually without the appearance of any new bands. Further examination reveals that the intensity of these bands in three samples shows a reduction in a similar proportion. Therefore, it is inferred that DBMP probably was eliminated as a whole and no cracking of DBMP molecules occurred during the treatment. For the assignments of the bands please see Table 1 in Ref. [17]. The characteristic bands ascribed to methene (2843, 1465 cm^{-1}) and methine (1460 cm^{-1}) groups in DBMP nearly can not be observed after the treatment at 673 K, suggesting the complete removal of DBMP [23–28]. In addition, the GC-MS results of the liquid trapped during the preparation of TiMPF, ZrMPF and AMPF show that DBMP is the main component, further confirming the removal of DBMP in the molecular form by vacuum evaporation, in accordance well with the above FT-IR results.

After thermal treatment at 773 K, the bands coming from CH_3PO_3 (2994 ~2934 cm^{-1} υCH_3; 1311 cm^{-1} δas P-CH_3; 1418 cm^{-1} δas P-CH_3) were still observed in the spectra of three samples, which could be taken as a proof that the hybrid structure of porous metal methylphosphonates has high thermal stability.

It is noteworthy to note that the symmetric bending vibration of P-CH_3 of CH_3PO_3 in both TiMPF and AMPF shifts to higher wavenumbers compared with that of TiMP and AMP, probably suggestting the existence of structural transformations during the removal of DBMP.

3.1.3. NMR

The ^{13}C CP/MAS NMR spectra of all samples are shown in Fig. 3. Five peaks at 63, 33, 19, 14 and 11 ppm can be observed for three as-synthesized metal methylphosphonates (TiMP, ZrMP and AMP). The former three peaks are assigned to O$\underline{C}H_2$, $\underline{C}H_2$, and $\underline{C}H_2CH_3$ in DBMP (labelled by underline), respectively. The latter two overlapping peaks could contain the other peaks in DBMP ($\underline{C}H_3$ and P$\underline{C}H_3$) and MPA (P$\underline{C}H_3$).

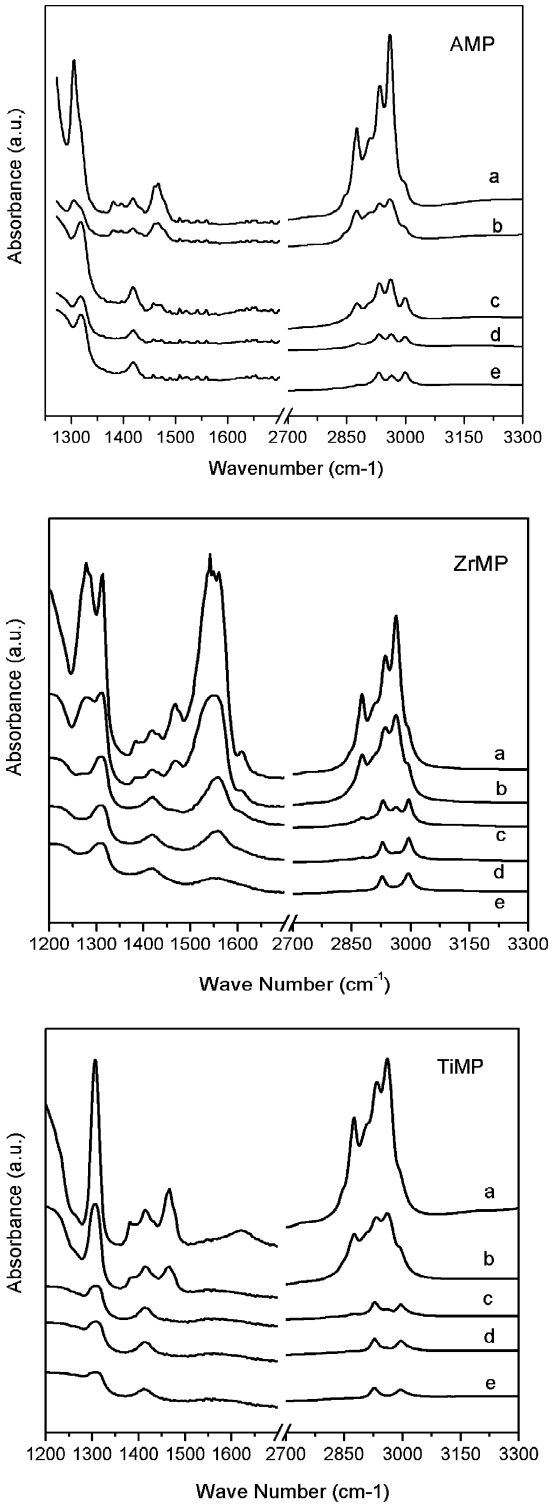

Fig. 2 FT-IR spectra of TiMP, ZrMP and AMP after treatment under vacuum at (a) room temperature (b) 523K (c) 623K (d) 673K (e) 773K

After the treatment under vacuum (673 K for AMP and 573 K for both TiMP and ZrMP), only one peak at 13 ppm,

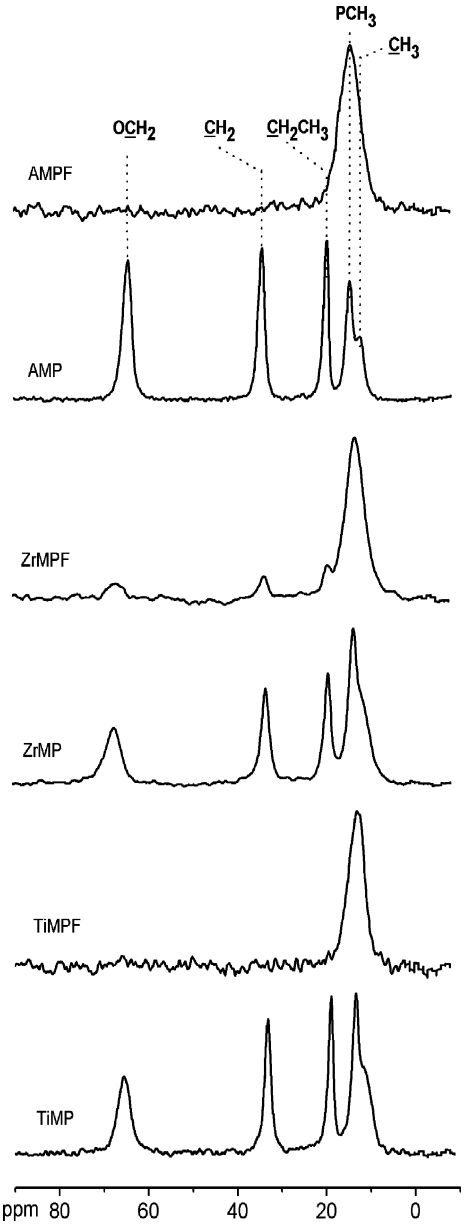

Fig. 3 ^{13}C CP/MAS NMR spectra of samples

assigned to the methyl group, presents in the spectra of TiMPF and AMPF. All peaks due to DBMP are absent, confirming the high efficiency of treatment method employed in this study. However, weak peaks arising from DBMP could still be observed in the spectrum of ZrMPF besides the strong peak at 13 ppm. This might be due to the lower treatment temperature, which caused the existence of DBMP residue. Comparing the peaks at 66, 33 and 19 ppm in the spectra of ZrMPF and ZrMP, one may find that the relative intensities of three peaks in two spectra are comparable. This suggests that DBMP is removed in the molecular form, in accordance with the above FT-IR results. Moreover, the broadness of the peak at 13 ppm for the final porous samples maybe implies

Table 2 TG results of TiMP, ZrMP and AMP samples

	Weight loss (wt%)		
Sample	(I)	(II)	(III)
TiMP	18.20	20.79	17.23
ZrMP	20.43	23.33	2.45
AMP	1.56	50.16	6.34

that the chemical environment of CH_3PO_3 changes accompanying the removal of DBMP.

Elemental analyses give H/C molar ratio of 2.92, 3.56 and 3.45 for TiMPF, ZrMPF and AMPF, respectively. These values are close to the theoretical H/C molar ratio of 3 in CH_3PO_3. Therefore, it is concluded that DBMP has been removed by the thermal treatment, whereas CH_3PO_3 is restrained in the structure of porous metal methylphosphonates.

3.1.4. Thermal analysis

Thermal analysis is used to study the thermal stability of metal methylphosphonates. TG and DTA curves of TiMP, ZrMP and AMP are shown in Fig. 4. The weight losses associated to each step of three samples are collected in Table 2.

In total, three stages of weight losses are expected in the TG curves of three samples. The initial weight loss below 400 K, corresponding to an endothermic process, is due to the water desorption. The second stage below 730 K gives a weigh loss of 2.79, 23.33 and 50.16 wt% for TiMP, ZrMP and AMP. Considering the characterization results of FT-IR and NMR, the exothermic weight loss in this range can be ascribed to the elimination of DBMP. The third weight loss, occurred after 753 K, should be relevant to the oxidation combustion of methyl group in CH3PO3. This implies that the hybrid structure of these porous organic-inorganic materials has high thermal stability.

Comparing the weight loss of three samples at different stages, AMP and TiMP show an unexpected large weight loss in the second stage and in the third stage, respectively. From Table 1, the total pore volume in AMP is about two times higher than those of TiMPF and ZrMPF, consistent well with the TG results. On the other hand, this also justifies the template role of DBMP during the synthesis. Moreover, the relatively high weight loss in TiMP due to CH_3PO_3 is in agreement with the elemental analysis of TiMPF, which contains higher amount of P and C.

3.2. Control samples synthesized without the use of DBMP

In order to further verify the templating effect of DBMP for the preparation of porous metal methylphosphonates, the

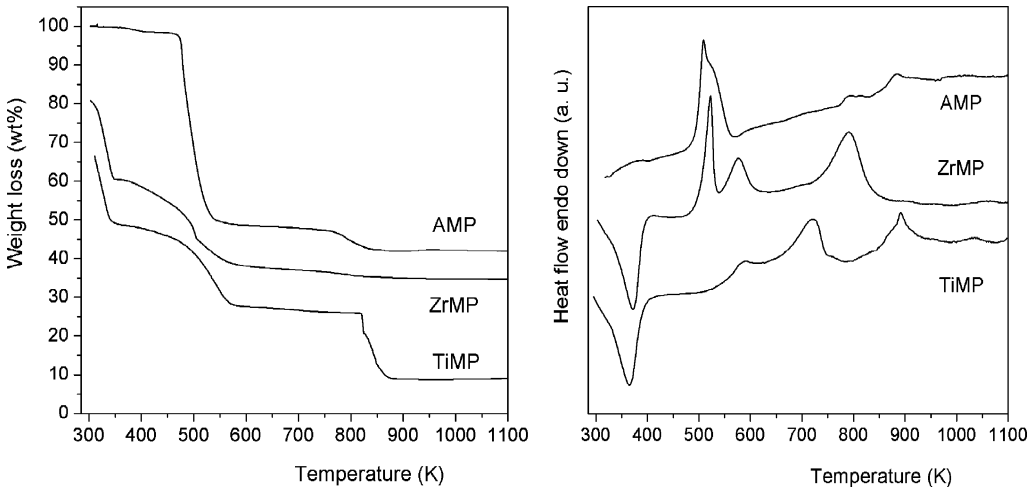

Fig. 4 TG (left) and DTA (right) curves of as-synthesized samples

control samples are prepared with the same procedures as those for TiMPF, ZrMPF and AMPF except the absence of DBMP.

Figure 5 gives the N_2 adsorption-desorption isotherms of TiMPcon, ZrMPcon and AMPcon. Judging from the isotherms of TiMPcon and AMPcon, both of them are non-porous materials with extremely small specific surface areas (see Table 1). Comparing the porous parameters of TiMPF and AMPF with their control samples, it is therefore evident to conclude that DBMP has played an important role in the formation of porous Ti and Al methylphosphonates, i.e. DBMP might act as a template during the synthesis.

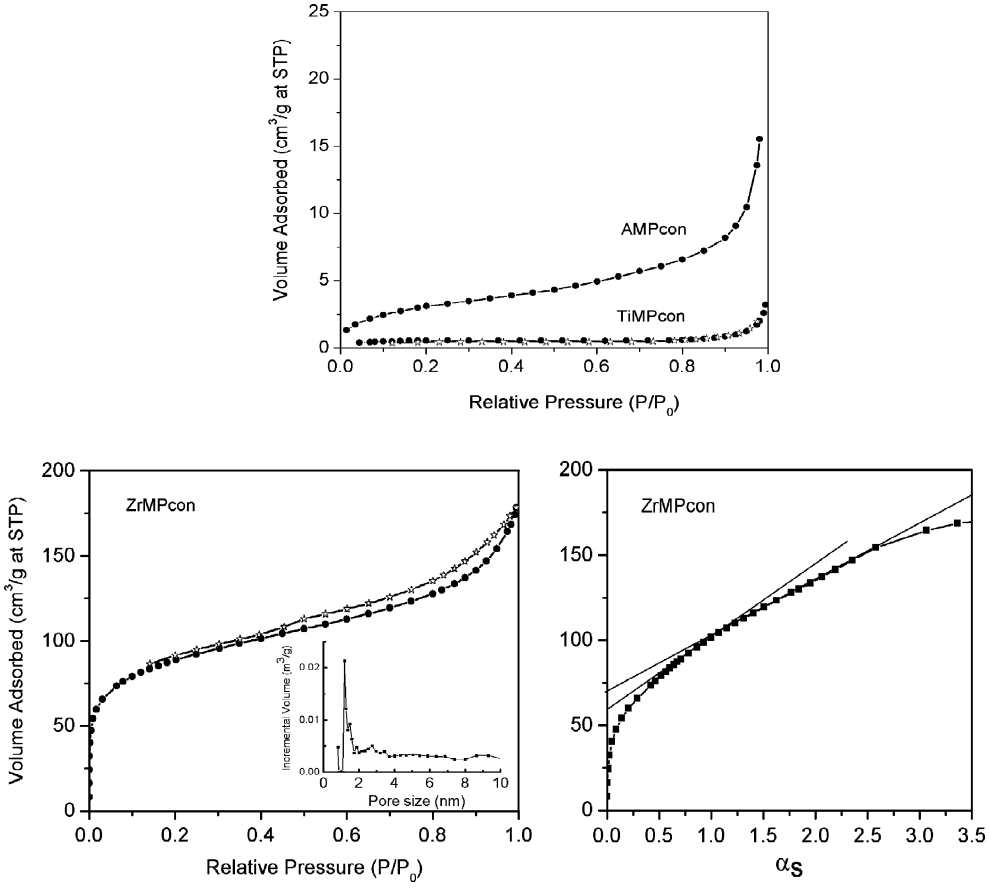

Fig. 5 N_2 adsorption-desorption isotherms (• adsorption, ⋆ desorption), pore size distribution (inset-by DFT method) and α_s plots of control samples

For ZrMPcon, the shape of the adsorption isotherm can be considered as a mixture of *Type I* and *Type II* isotherms. The initial part of the adsorption isotherms shows a steep rise assigned to microporous filling, and the slope of the plateau at highly relative pressure is due to multilayer adsorption on mesoporous, macroporous or external surface. The shape of the hysteresis loop is of typical of *Type H4*, indicating that ZrMPcon consists of slit-shaped pores with the PSD mainly in the microporous range. The PSD calculated using DFT method gives a broad peak with the maximum at 1.18 nm. The α_s plot of ZrMPcon also gives an upward swing at $0 < \alpha_s < 0.75$, which suggests the existence of micropores in the structure. Additionally, there are two linear regions locating at $0.8 < \alpha_s < 1.5$ and $1.75 < \alpha_s < 2.5$, respectively. V_{mi} and the sum of S_{me} and S_{ext} are calculated from the intercept and slope of the former linear region. The sum of V_{mi} and the mesoporous volume (V_{me}) and S_{ext} are calculated from the intercept and slope of the latter linear region [22, 29].

The large specific surface area and porous structure of ZrMPcon complicate the templating effect of DBMP. There are micropores and mesopores in the structure of ZrMPcon. Based on its nitrogen adsorption-desorption isotherm and hysteresis loop, it could be deduced that the slit-shaped micropore plays a leading role in the structure of ZrMPcon. Therefore, the stacking of unequally sized layers could be the source of the micropores [30, 31]. The other reported zirconium methylphosphonates show the *Type II* isotherms with little or no hysteresis loop at relative pressure below 0.7, which indicates that there are few mesopores. The high specific surface area is mainly due to the micropores produced by the stacking of layers [31]. However, the nitrogen adsorption-desorption isotherm of ZrMPF is of *Type I* and only micropore exists in the structure. These observations rationalize the assignment of the templating-effect of DBMP, by which the porous structure of zirconium methylphosphonate is formed.

4. Conclusions

DBMP is a nice template for preparing porous metal methylphosphonates, and can be easily removed in the molecular form from the structures of as-synthesized samples through thermal treatment under vacuum. Thermal analysis and FT-IR results reveal that the hybrid structures of porous TiMPF, ZrMPF and AMPF are thermally stable up to 773 K. Moreover, a structure transformation might occur during thermal treatment of AMP, as confirmed by FT-IR spectra and ^{13}C CP/MAS NMR.

The present synthetic method is promising for the preparation of stable organic-inorganic hybrid porous materials. The next concern would be the synthesis of novel porous metal alkylphosphonates with other neutral phosphonates as templates, the investigation of the structural transformation during the postsynthesis treatment and the exploration of the interactive mechanism between template and framework, which could be very instructive for the design of novel materials.

References

1. C.S. Cundy and P.A. Cox, Chem. Rev. **103**, 663 (2003).
2. K.J.C. van Bonnel, A. Friggeri, and S. Shinkai, Angew. Chem. Int. Ed. **42**, 980 (2003).
3. G.J. de, A.A. Soler-lllia, C. Sanchez, B. Lebeau, and J. Patarin, Chem. Rev. **102**, 4093 (2002).
4. H. Gies and B. Marler, Zeolites. **12**, 42 (1992).
5. B.M. Lok, T.R. Cannan, and C.A. Messina, Zeolites. **3**, 282 (1983).
6. C. Kresge, M. Leonowicz, W. Roth, J. Vartuli, and J. Beck, Nature. **359**, 710 (1992).
7. U. Ciesla and F. Schuth, Microporous Mesoporous Mater. **27**, 131 (1999).
8. J.L. Blin, A. Léonard, Zh. Y. Yuan, L. Gigot, A. Vantomme, A.K. Cheetham, and B.L. Su, Angew. Chem. Int. Ed. **42**, 2872 (2003).
9. R. Ryoo, S.H. Joo, and S. Jun, J. Phys. Chem. B, **37**, 7743 (1999)
10. S. S. Yoon, J. Y. Kim, and J. S. Yu, Chem. Commun., 559 (2001).
11. J.Y. Kim, S.B. Yoon, and J.S. Yu, Chem. Mater. **15**, 1932 (2003).
12. A.P. Wight and M.W. Davis, Chem. Rev. **102**, 3589 (2002).
13. P.J. Langley and J. Hulliger, Chem. Soc. Rev. **28**, 279 (1999).
14. B. Moulton and M.J. Zaworotko, Current Opinion in Solid State and Mater. Sci. **6**, 117 (2002).
15. J.W. Johnson, J.F. Brody, and R.M. Alexander, Chem. Mater. **2**, 198 (1990).
16. J.W. Johnson, A.J. Jacobson, W.M. Butler, S.E. Rosenthal, J.F. Brody, and J.T. Lewandowski, J. Am. Chem. Soc. **111**, 381 (1989).
17. Z.B. Wu, Zh. M. Liu, P. Tian, Y.L. He, L. Xu, X.M. Liu, X.H. Bao, and X. Ch. Liu, Microporous Mesoporous Mater. **62**, 61 (2003).
18. S.J. Gregg and K.S.W. Sing, Adsorption, Surface Area and Porosity, 2nd ed., Academic Pressure: London, 1982.
19. K. Kaneko, C. Ishii, H. Kanoh, Y. Hanzawa, N. Setoyama, and T. Suzuki, Adv. Colloid Interface Sci. **76–77**, 295 (1998).
20. M. Kruk, V. Antochshuk, and M. Jaroniec, J. Phys. Chem. B **103**, 10670 (1999).
21. F. Rouquerol, J. Rouquerol, and K. Sing, Adsorption by Powders and Porous Solids, Academic Press: UK, 1999.
22. N. Setoyama, T. Suzuki, and K. kaneko, Carbon **36**, 1459 (1998).
23. K. Maeda, Y. Kiyozumi, and F. Mizukami, J. Phys. Chem. B **101**, 4402 (1997).
24. C. Li, Q. Xin, K.L. Wang, and X.X. Guo, Applied Spectros. **45**, 874 (1991).
25. M. Rokita, M. Handke, and W. Mozgawa, J. Mol. Struc. **450**, 213 (1998).
26. L. Bertilsson, K.P. Kamloth, H.D. Liess, I. Engquist, and B. Liedberg, J. Phys. Chem. B **102**, 1260 (1998).
27. L.X. Cao, S.R. Segal, S.L. Suib, X. Tang, and S. Satyapal, J. Catal. **194**, 61 (2000).
28. H.R. Watling, P.M. Sipos, L. Byrne, G.T. Hefter, and P.M. May, Appl. Spectr. **53**, 415 (1999).
29. Z.M. Wang, K. Hoshinoo, K. Shishibori, H. Kanoh, and K. Ooi, Chem. Mater. **15**, 2926 (2003).
30. M.B. Dines and P.C. Griffith, J. Phys. Chem. **86**, 571 (1982).
31. A. Clearfield, Prog. Inorg. Chem. **47**, 371 (1998).